

Immunocytochemical Localization of NTPDases 1 and 2 in the Neural Retina of Mouse and Zebrafish.

María Jimena Ricatti, Lionel D. Alfie, Élise G. Lavoie, Jean Sévigny, Pablo J. Schwarzbaum, and María Paula Faillace.

Cita:

María Jimena Ricatti, Lionel D. Alfie, Élise G. Lavoie, Jean Sévigny, Pablo J. Schwarzbaum, and María Paula Faillace (2009). *Immunocytochemical Localization of NTPDases 1 and 2 in the Neural Retina of Mouse and Zebrafish*. *SYNAPSE*, 63 (4), 291-307.

Dirección estable: <https://www.aacademica.org/lionel.david.alfie/14>

ARK: <https://n2t.net/ark:/13683/pux8/UN6>



Esta obra está bajo una licencia de Creative Commons.
Para ver una copia de esta licencia, visite
<https://creativecommons.org/licenses/by-nc-nd/4.0/deed.es>.

Acta Académica es un proyecto académico sin fines de lucro enmarcado en la iniciativa de acceso abierto. Acta Académica fue creado para facilitar a investigadores de todo el mundo el compartir su producción académica. Para crear un perfil gratuitamente o acceder a otros trabajos visite: <https://www.aacademica.org>.

Immunocytochemical Localization of NTPDases 1 and 2 in the Neural Retina of Mouse and Zebrafish

MARÍA JIMENA RICATTI,¹ LIONEL D. ALFIE,¹ ÉLISE G. LAVOIE,² JEAN SÉVIGNY,²
PABLO J. SCHWARZBAUM,³ AND MARÍA PAULA FAILLACE^{1,3*}

¹Departamento de Fisiología, Facultad de Medicina, Universidad de Buenos Aires, C1121ABG, Ciudad Autónoma de Buenos Aires, Argentina

²Centre de Recherche en Rhumatologie et Immunologie, Centre Hospitalier Universitaire de Québec, Université Laval, Québec, Canada G1V4G2

³IQUIFIB, Facultad de Farmacia y Bioquímica, Universidad de Buenos Aires, C1113AAD, Ciudad Autónoma de Buenos Aires, Argentina

KEY WORDS ectonucleotidases; NTPDase; zebrafish; mouse; retina; ATP; ADP; extracellular nucleotides

ABSTRACT Ectonucleoside triphosphate diphosphohydrolases (E-NTPDases) are a family of membrane-bound enzymes that hydrolyze extracellular di- and triphosphate nucleosides. E-NTPDases have been proposed to control extracellular nucleotide levels that mediate intercellular communication by binding to specific membrane receptors. Here we show a detailed immunocytochemical localization of two enzymes of the E-NTPDase family in the retinal layers of two vertebrate species, namely, the mouse and the zebrafish. In the mouse retina, NTPDase2 was chiefly localized in Müller glia and ganglion cell processes. NTPDase1 was located on neurons as well, since it was expressed by horizontal and ganglion cell processes, suggesting that nucleotides such as ATP and ADP can be hydrolyzed at the surface of these cells. NTPDase1 was also detected in intraretinal blood vessels of the mouse. Regarding zebrafish, NTPDases1 and 2 seem to be differentially localized in horizontal cell processes, photoreceptor segments, and ganglion cell dendrites and axons, but absent from Müller glia. Moreover, NTPDases1 and 2 appear to be expressed within the germinal margin of the zebrafish retina that contains proliferative and differentiating cells. Retinal homogenates from both species exhibited ecto-ATPase activity which might be attributed at least to NTPDases1 and 2, whose expression is described in this report. Our results suggest a compartmentalized regulation of extracellular nucleotide/nucleoside concentration in the retinal layers, supporting a relevant role for extracellular nucleotide mediated-signaling in vertebrate retinas. **Synapse 63:291–307, 2009.** © 2008 Wiley-Liss, Inc.

INTRODUCTION

Ectonucleoside triphosphate diphosphohydrolases, also known as E-NTPDases, belong to a family of membrane-bound enzymes that hydrolyze the terminal γ and β phosphate residues of nucleotides, such as ATP, ADP, UTP, and UDP. NTPDases play an important role in controlling several autocrine and paracrine signaling events mediated by extracellular nucleotides, by regulating ligand concentration at specific purinergic or “P” receptors (Burnstock, 1978, 2007; Lazarowski et al., 2003). At present, eight genes for the E-NTPDase family have been cloned in vertebrate tissues. They contain five highly conserved DNA sequence domains named “apyrase conserved regions.” NTPDases1, 2, 3, and 8 are plasma mem-

brane enzymes with their catalytic site placed extracellularly, whereas the four remainder NTPDases are positioned in intracellular organelles and hydrolyze

Contract grant sponsor: Agencia Nacional de Promoción Científica y Tecnológica (ANPCyT); Contract grant numbers: BID1728/04-PICT2004, 25422; Contract grant sponsor: Consejo Nacional de Investigaciones Científicas y Técnicas (CONICET); Contract grant numbers: PIP2004, 6012; Contract grant sponsor: Fundación Antorchas; Contract grant number: 14306-6; Contract grant sponsor: ANPCyT; Contract grant number: 1432; Contract grant sponsors: UBA, CONICET.

*Correspondence to: María Paula Faillace, Laboratorio de Neurociencia, Departamento de Fisiología, Facultad de Medicina, Paraguay 2155 7° piso, C1121ABG, Ciudad Autónoma de Buenos Aires, Argentina.
E-mail: pfaillace@qb.ffyb.uba.ar

Received 13 June 2008; Accepted 11 August 2008

DOI 10.1002/syn.20605

Published online in Wiley InterScience (www.interscience.wiley.com).

nucleotides other than ATP or ADP (Fausther et al., 2007; Mulero et al., 1999; Trombetta and Helenius, 1999; Wang and Guidotti, 1998). In several cell systems, plasma membrane NTPDases together with an ecto 5'-nucleotidase (hydrolyzes AMP to adenosine) constitute a catabolic cascade which completely dephosphorylates extracellular ATP to adenosine (Hunsucker et al., 2005; Zimmermann, 2006). Therefore, extracellular hydrolysis of triphosphate nucleotides not only ends their action on specific receptors but produces other molecules that are in turn receptor-mediated extracellular signals. In the central nervous system, considerable evidence exists indicating that ATP is released from neurons and glia to the extracellular milieu, where the nucleotide acts both as a neurotransmitter and a precursor for adenosine. Adenosine can in turn activate signaling pathways (Burnstock, 1972; Fellin et al., 2006; Newman, 2006). Thus, extracellular nucleotides trigger signaling pathways that are important for neuron–glia interactions (Newman, 2006; Newman and Zahs, 1998). Recent studies suggest that NTPDases are important for degradation of extracellular ATP within the retina. In fact, extracellular ATP hydrolysis products regulate ganglion cells (GCs) hyperpolarization as well as calcium wave propagation in glial cells (Newman, 2006). Noteworthy, NTPDase2 overexpression induces ectopic eyes, whereas its downregulation abolishes eye and retina formation in *Xenopus laevis* embryos (Massé et al., 2007). However, only one recent report has described the presence of NTPDases in the retina of rat (Iandiev et al., 2007).

The vertebrate neural retina is an ordered and stratified tissue with six neural cells (cone and rod photoreceptors; interneurons represented by horizontal, bipolar, and amacrine cells; and projection neurons called ganglion cells) and a specific type of glia, the Müller cell (Dowling, 1979; Ramón y Cajal, 1892). Neurons are stratified in different synaptic layers and form a laminar array characteristic of the vertebrate retina (Fadool and Dowling, 2008; Masland, 2001). In addition, cells are arranged in ordered mosaics that endow retinal layers with an accurate representation of the visual field (Cameron and Carney, 2000; Wässle and Riemann, 1978).

The aim of the present report is to describe the distribution of two members of the E-NTPDase family in retinal cells and synaptic layers. We opted for NTPDase1 and NTPDase2 because they both regulate extracellular nucleotide levels, but NTPDase1 exhibits a similar capacity for hydrolyzing triphosphate as well as diphosphate nucleosides, whereas NTPDase2 has a 30-fold preference for the hydrolysis of ATP over ADP (Kaczmarek et al., 1996; Kukulski et al., 2005). Therefore, when NTPDase1 is expressed a faster inactivation of P2 receptors is expected, together with adenosine synthesis and activation of P1

receptors (Burnstock, 1978, 2007; Freedholm, 1995). In contrast, when NTPDase2 is present ADP accumulates and adenosine production is delayed (Kukulski et al., 2005). Information about NTPDases localization in the retinal layers described here provides insight into the compartmentalized regulation of extracellular ATP/ADP concentration. Furthermore, the present study examines similarities and variations of the retinal distribution of NTPDases1 and 2 between a teleost fish and a rodent. This is of interest because, although these animals' retina exhibits similar architectural, genetic, and functional features, zebrafish can grow and regenerate all retinal cells during the animal's life span (Raymond et al., 2006), whereas mouse retina loses this capacity soon after birth.

MATERIALS AND METHODS

Animals

Zebrafish (*Brachydanio rerio*) were obtained from a local aquarium (Ichthys, Buenos Aires, Argentina) and maintained indoors at 28.5°C, exposed to 14/10-h light/dark cycle for at least 3 weeks. They were fed twice a day with freshly hatched *Artemia* sp. and dry food for tropical fish. For immunocytochemical and enzyme activity assays, 3-month-old adult zebrafish of about 3 cm in body length and 1.5 g of weight were anesthetized by immersion in ice-cold MS-222 solution (0.02%, w/v), then decapitated and enucleated on ice.

Male mice weighing 20–23 g (*Mus musculus*, SWISS strain) were obtained from the Animal Care Facility at the School of Pharmacy and Biochemistry, University of Buenos Aires (Buenos Aires, Argentina). Animals were maintained under a 14/10-h light/dark cycle and fed ad libitum. Mice were deeply anesthetized with a mixture of ketamine–xylazine (100 mg/kg of animal–15 mg/kg, IP), and once animals were totally unresponsive to painful stimuli, they were exanguinated by intracardiac perfusion with 0.9% saline followed by paraformaldehyde 4% in PBS at pH 7.4. For enzyme activity assays, mice were first anesthetized with a lethal dose of the anesthetic mixture and then decapitated and enucleated. The Committee on Animal Research at University of Buenos Aires approved protocols for animal use and care.

Exposure to 5-bromo-2'-deoxyuridine

Animals were exposed to 5-bromo-2'-deoxyuridine (BrdU; Sigma, St. Louis, MO). This nucleotide analog intercalates in the DNA during the S phase of the cell cycle. To sustain a high systemic level of BrdU, 5–6 zebrafish were maintained in 250 mL of water containing BrdU (2 g/L) and neutral regulator (0.08 g/L; SeaChem Laboratories, Stone Mountain, GA). Water in the tank was kept at 28.5°C and aerated. Zebrafish

TABLE I. List of primary antibodies against NTPDase1 and NTPDase2 used in this study

Rabbit polyclonal anti-NTPDase1 antibodies	Peptide sequences for generation of rabbit antibodies	% of homology with human NTPDase1 sequence	% of homology with mouse NTPDase1 sequence	% of homology with zebrafish NTPDase1 sequence
mN1-kaly (KY102/130) and mN1-K2B3	GIYLTDCME RAREVIPRSQHQ ETPVYLGA	GIYLTDCME RAREVIPRSQHQ ETPVYLGA	GAYLAECME LSTELIPTS KHH QTPVYLGA	GASLEECMK EAKEKIPARRHS ETPVYLGA
	Human CD39 amino acid sequence 102–130	100%	62.06%	58.62%
RO202/217	KSDTQETY GALDLGGA	ETNNQETF GALDLGGA	DSQKQETF GALDLGGA	LRKPAGTL GALDLGGA
	Porcine CD39 amino acid sequence 202–217	68.75%	75%	56.25%
Rabbit polyclonal anti-NTPDase2 antibody (mN2-36)	Immunogen injected: cDNA of the whole gene for the mouse NTPDase2 ligated into pcDNA3			

List of primary antibodies used as retinal markers in this study

Anti-postsynaptic density 95 kDa (PSD95)	Monoclonal antibody is a presynaptic marker labeling cone and rod pedicles in the retina of mouse (Koulen et al., 1998). This antibody did not label zebrafish retinas (our unpublished observations). Dilution: 1:400 (clone K28/43; Upstate, Lake Placid, NY).
Anti-protein kinase C α/β (PKC α/β)	Monoclonal antibody recognizes all ON bipolar cells in zebrafish (Yazulla and Studholme, 2001) and rod-driven ON bipolar cells in mouse (Greferath et al., 1990; Haverkamp and Wässle, 2000). Dilution: 1:100 (clone MC5; Santa Cruz Biotechnology, Santa Cruz, CA).
Anti-SV2	Monoclonal antibody is a marker of presynaptic vesicles in both OPL and IPL. Dilution: 1:2000 (Yazulla and Studholme, 2001; Developmental Studies Hybridoma Bank, Iowa, IA).
Anti-zns-2	Monoclonal antibody recognizes cone photoreceptors in zebrafish (Larison and Trevarrow, 1994; Yazulla and Studholme, 2001). Dilution: 1:100 (Developmental Studies Hybridoma Bank).
Anti-RT97	Monoclonal antibody recognizes polyphosphorylated epitopes on neurofilaments and other molecules such as rhodopsin (Anderton et al., 1982). In mouse retina, this antibody mainly labeled processes of horizontal cells and axons of ganglion cells (Dräger et al., 1984; Inoue et al., 2002). In zebrafish retina, strong labeling was observed in rod and cone photoreceptor outer segments (Adamus et al., 1988). Dilution: 1:500 (Developmental Studies Hybridoma Bank).
Anti-tyrosine hydroxylase	Monoclonal antibody labels dopaminergic amacrine and interplexiform cell processes in both the IPL and OPL (Haverkamp and Wässle, 2000; Yazulla and Studholme, 2001). Dilution: 1:200 (Chemicon Int., Temecula, CA).
Anti-glutamine synthetase	Monoclonal antibody labeled throughout Müller cell bodies. Dilution: 1:200 (BD Biosciences, San Jose, CA).
Anti-BrdU	Monoclonal antibody was used to detect the nucleotide analogue incorporated in the nuclei of mitotically active cells. Dilution: 1:200 (Roche, Indianapolis, IN).

were maintained in the nucleotide analog-containing water for 48 h and then washed with fresh water and immediately euthanized.

Tissue processing

Enucleated eyes either from mice or zebrafish were dissected to prepare eyecups. Cornea, lens, and vitreous were carefully removed preserving the retina. Eyecups were fixed with 4% paraformaldehyde in PBS (137 mM NaCl, 2.7 mM KCl, 5.7 mM phosphate, pH 7.4) for either 1 h (zebrafish) or 30 min (mice), and then the fixative was carefully washed several times with 5% sucrose in PBS, incubated for 30 min in 10% sucrose in PBS, and finally incubated overnight with a similar solution containing 20% of sucrose. Then, eyecups were embedded in Jung tissue freezing medium (Leica Microsystems, Nussloch, Germany) and frozen in dry ice. Ten-micrometer frozen sections were cut at -20°C with a cryostat. Sections were collected onto gelatin subbed-slides and kept at -20°C until use.

Immunocytochemistry

Slides containing eyecup sections were dried at 50°C for 10 min, allowed to cool at room temperature, hydrated in PBS-T (PBS plus 0.1% Tween-20), and held in 5% normal goat serum (NGS; Vector Laboratories, Burlingame, CA) in PBS-T for 1 h at room temperature. Sections were then incubated overnight with primary either mouse monoclonal or rabbit polyclonal antibodies in 3% NGS in PBS-T (primary antibodies are listed in Table I) in a humid chamber at 4°C . Slides were washed four times with PBS-T and then incubated in darkness for 2 h at room temperature, with secondary antibodies against either mouse or rabbit antibodies made in goat and conjugated to ALEXA 488 or 546 (Invitrogen, Carlsbad, CA; 1:400 in 3% NGS in PBS-T). Finally, sections were washed and coverslipped with mounting medium for fluorescence (Vector Laboratories). For double labeling assays, eyecup sections were incubated in 3% NGS in PBS-T containing both primary and, after washing, secondary antibodies.

For colocalization studies of NTPDase1 or NTPDase2 with each retinal marker, four to five different animals (either mouse or zebrafish) were assessed.

Control sections for immunoreactions

1. Reaction with preimmune sera from preinoculated rabbits (for either mN1-kaly or mN2-36 antibodies), used at identical dilutions and instead of specific primary antibodies.
2. Omission of either primary or secondary antibody. In double labeling assays, either one or two primary and either one or two secondary antibodies were alternatively omitted from control slides.

Characterization of primary antibodies

The three primary polyclonal antibodies against NTPDase1, namely, RO202/217, KY102/130 (named mN1-kaly), and mN1-K2B3, were assayed (Table I). These antibodies gave a similar pattern of labeling both in zebrafish and mouse (data not shown). Subsequent experiments were performed with mN1-kaly that showed less background.

To generate polyclonal antibodies KY102/130 and K2B3, a high-density multigenic peptide system (MAPS) was synthesized with peptides corresponding to amino acid sequence 102–130 of human CD39 (Table I). This approach used a small peptidyl core matrix of four lysine residues bearing four branching peptides (Service de séquence de peptide de l'Est du Québec). KY102/130 and K2B3 correspond to serum collected and characterized from different rabbits (Schulte am Esch et al., 1999).

RO202/217: A 16 amino acid peptide from the N-terminus of the porcine pancreatic NTPDase1 (Table I) was used for the generation of this rabbit polyclonal antibody. This polyclonal antibody preparation has been found to react with human CD39/ATPDase (NTPDase1) expressed by COS-7 transfectants, but it does not exhibit crossreactivity with NTPDase2 (Schulte am Esch et al., 1999).

mN2-36: Antimurine NTPDase2 polyclonal antibody (Table I) was raised in rabbits by injection of complementary DNA encoding the whole gene for the murine NTPDase2 ligated into pcDNA3. Serum titers were determined by standard western blot analysis under nonreducing conditions in the screening protein lysates from COS-7 cells expressing recombinant murine NTPDase2 (Sévigny et al., 2002). Immunocytochemical studies in neural and nonneural tissues of rat and mouse demonstrated that this antibody specifically detects NTPDase2 and does not crossreact with NTPDase1 (Enjyoji et al., 1999; Mishra et al., 2006; Shukla et al., 2005; Vlajkovic et al., 2002).

Microscopy and image analysis

Fluorescent cell images were captured with a confocal microscope (model LSM 5 PASCAL EXCITER; Carl Zeiss, Germany) by using 40×/1.3 and 63×/1.4 objectives. LSM 5 Image Browser software (Carl Zeiss LSM Data Server) and Adobe Photoshop version CS2 were used for digital processing of images.

Ecto-ATPase activity

The measurements of the ecto-ATPase activity were performed by monitoring the rate of ATP hydrolysis in retinal homogenates. Briefly, retinas from either mouse or zebrafish were carefully separated from eye-cups, freed of retinal pigmented epithelium (RPE), and homogenized in a reaction medium containing 30 mM Tris-HCl (pH 7.4), 5 mM KCl, 100 mM NaCl, 4 mM CaCl₂, and 1 mM PMSF, chilled on ice. Zebrafish were dark adapted for 1 h to allow complete separation of RPE from the neural retina. Homogenates from the retina of both species were centrifuged at 15,000g during 30 min at 4°C and pellets were again homogenized in 1 mL of reaction medium without PMSF. The resulting extract was denoted as “centrifuged homogenate.” ATPase activity was measured either in the absence (total ATPase activity) or presence (ecto-ATPase activity) of the following inhibitors: 10 μM vanadate, 2 μg/mL oligomycin, 1 mM *N*-ethylmaleimide, and 1 mM levamisol (Sigma). Vanadate, oligomycin, and *N*-ethylmaleimide inhibit ATPases of type P, F, and V, respectively, whereas levamisol inhibits alkaline phosphatases. In addition, ATPase activity was assayed in the presence of the aforementioned inhibitors and 10 mM either EDTA or cibacron blue 3GA (Sigma). ATPase activity was determined by following the time course of [³²P]Pi release from [³²P]-ATP at 25°C (Schwarzbaum et al., 1998). In brief, reactions were started by adding [³²P]-ATP (NEN Life Science Products, Boston, MA) to the “centrifuged homogenate” under stirring. Final concentration of ATP was 2 mM and specific activity of [³²P]-ATP was 450–900 mCi/mol of ATP. At different times, a 50 μL aliquot was withdrawn from the reaction and poured into 750 μL of a stop solution containing 4.05 mM Mo₇O₂₄(NH₄)₆ and 0.83 mM HClO₄. The resultant ammonium molybdate–phosphate complex was next extracted by adding 600 μL of isobutyl alcohol under vigorous stirring. Then, phases were separated by centrifugation for 5 min at 1000 g. Aliquots (200 μL) of the organic phase that contains [³²P]Pi were transferred to vials with 2 mL of 0.5 M NaOH and then radioactivity was measured. Fifty microliters of aliquots contained 80–100 μg of proteins (Lowry et al., 1951).

To calculate the initial rate values (*v*_i), the following equation was fitted to the experimental data:

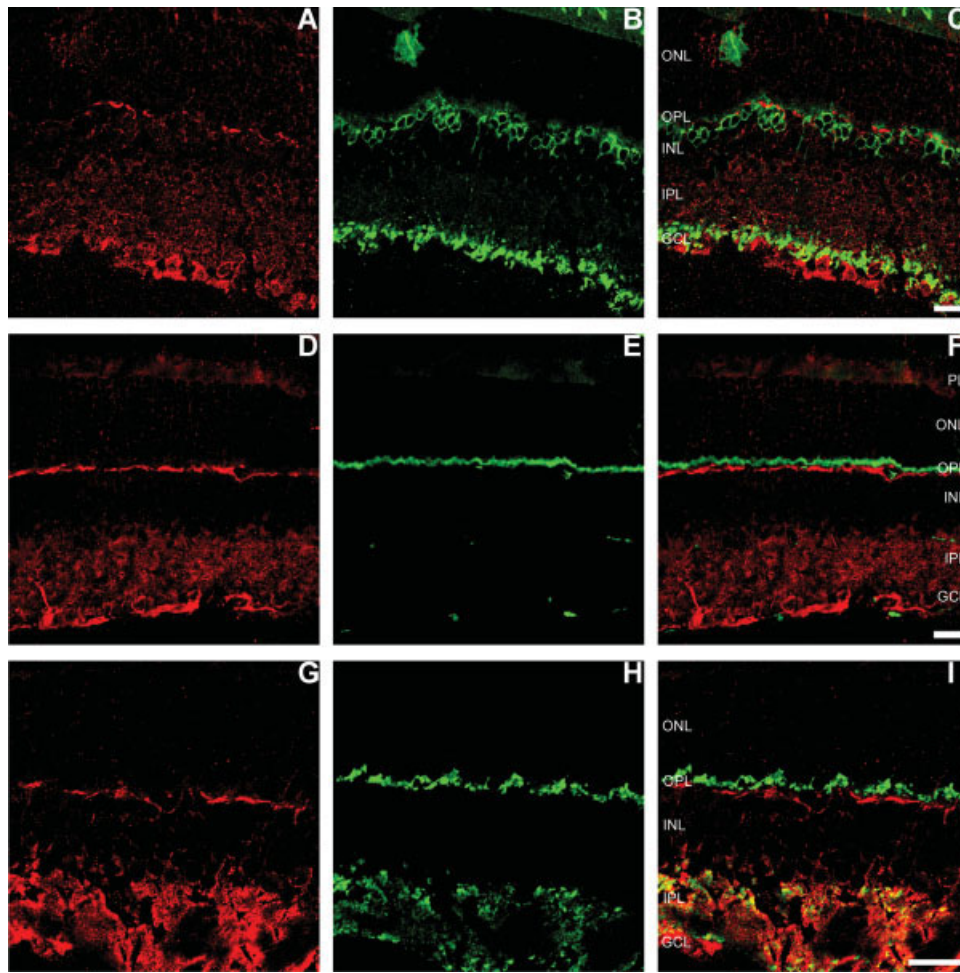


Fig. 1. Confocal microscopic images of transverse sections from mouse retinas. NTPDase1 immunoreactivity (IR) is labeled red (A, D, G) and retinal markers are shown in green. PKC α/β -labeled ON bipolar cells are shown in B. Panel E shows PSD95-labeled photoreceptor feet. Panel H depicts SV2-labeled presynaptic vesicles in the outer plexiform (OPL) and inner plexiform layers (IPL). Images from each row were overlaid in the third column. In the OPL,

NTPDase1-labeling follows a postsynaptic pattern (panel F), but it is not on bipolar dendrites (panel C). In the IPL, however, partial colabeling is observed between NTPDase1 and the presynaptic vesicle marker (panel I). PL, photoreceptor layer; ONL, outer nuclear layer; INL, inner nuclear layer; GCL, ganglion cell layer. Images in the same row show identical magnification. Scale bars = 20 μ m.

$Y = Y_0 + A(1 - e^{-kt})$, where Y and Y_0 are the values of Pi at any time (t) and $t = 0$, respectively. The parameter A represents the maximal value for the increase of Y with time, whereas k is a rate coefficient. The parameters of best fit from the regression were used to calculate enzyme activity (v_i) as kA , i.e., the first derivative of the equation for t tending to zero. Activity data (v_i) are mean \pm SD and are expressed as nmol/(μ g protein \cdot min).

RESULTS

Localization of NTPDase1 and NTPDase2 by immunocytochemistry

In all figures, immunoreactivity (IR) for NTPDase antibodies is shown in red, while that for cell-type

retinal markers is displayed in green. The third column was obtained by overlapping two confocal images from identical microscopic fields. Colocalization was considered positive when yellow color formed as a result of superimposing green and red images from the same microscopic field.

NTPDase1 in the mouse retina

Since antibodies against NTPDase1 label blood vessels in other tissues, we searched for positive IR in the choroid, the vascular layer of the eye. We consistently observed labeled vascular vessels in this tissue both in mouse and zebrafish eyecup sections.

Regarding mouse neural retina, IR of mN1-kaly shows a sharp thin band in the outer plexiform layer

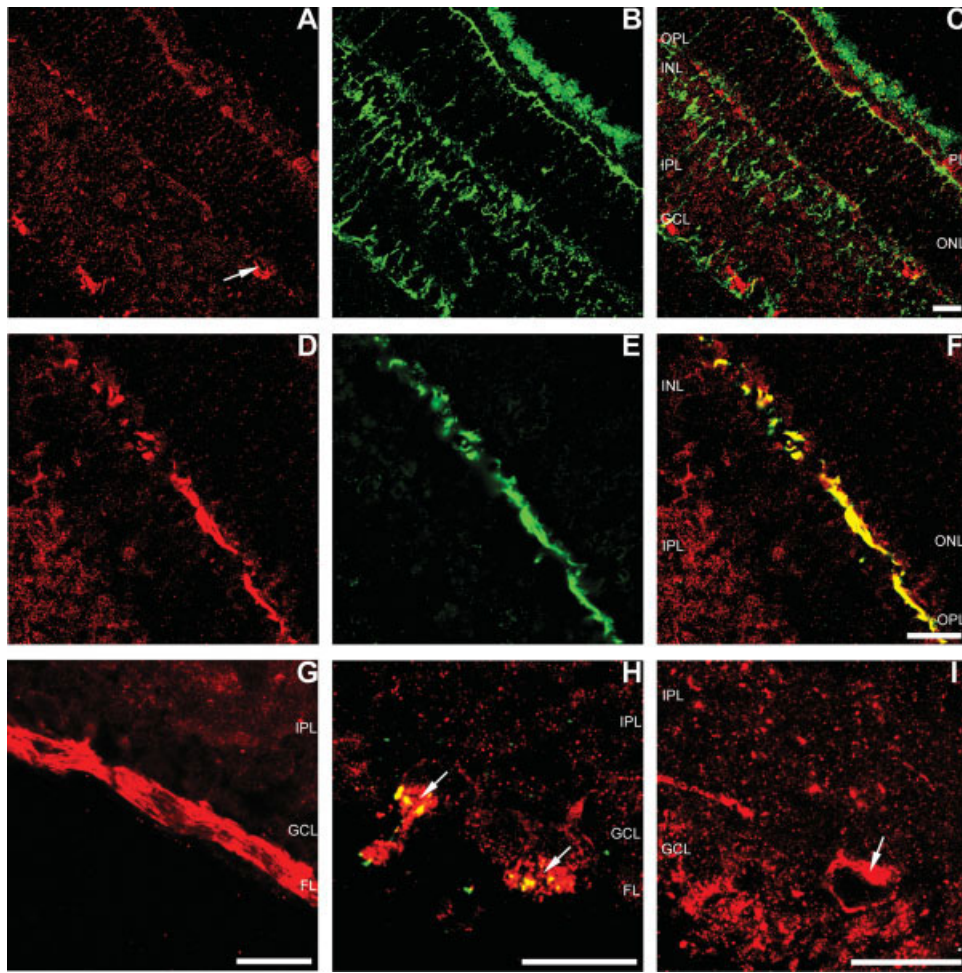


Fig. 2. Confocal microscopic images of transverse sections from mouse retinas. NTPDase1 immunoreactivity (IR) is labeled red (A, D, G, I) and retinal markers are shown in green. Glutamine synthetase-labeled Müller cells (B) and RT97-labeled horizontal cells in the outer plexiform layer (OPL) (E). Images from each row are superimposed in C and F. Panel H depicts an overlaid image of RT97- and NTPDase1-IR in the ganglion cell (GC) and fiber layers (FL). Complete colabeling in the OPL (F) and partial colabeling in

H (arrows) indicate the presence of NTPDase1-IR in horizontal cell processes as well as GC axons. NTPDase1 immunoreactivity in axon bundles is also observed in G. Arrows in A and I show NTPDase1-IR in vascular vessel-like structures in the OPL and ganglion cell layer (GCL), respectively. PL, photoreceptor layer; ONL, outer nuclear layer; INL, inner nuclear layer; IPL, inner plexiform layer. Images in the same row show identical magnification. Scale bars = 20 μ m.

(OPL) and a diffuse and scattered labeling in the inner plexiform layer (IPL). An additional strong signal can be observed in the border of the vitreal surface (Figs. 1A, 1D, and 1G). In many mN1-kaly immunoreacted sections, a much fainter and punctate staining is present around some but not all cell bodies in both nuclear layers. The ON bipolar cell marker PKC α/β does not colocalize with NTPDase1 in bipolar cell either dendrites in the OPL, somas in the inner nuclear layer (INL), or synaptic terminals in the IPL (Figs. 1A–1C). In mouse retinas, PSD95 (Fig. 1E) labeled photoreceptor pedicles (see Table I). This marker does not show colocalization with NTPDase1-IR (Figs. 1D–1F). Likewise, double labeling by using mN1-kaly and SV2 antibodies does not evidence spa-

tial associations of NTPDase1 and the presynaptic vesicle marker in the OPL (Figs. 1G–1I). Thus, the absence of colocalization of NTPDase1 with both retinal markers suggests that in the OPL the enzyme is mainly located in postsynaptic processes. Furthermore, although partial colabeling is observed, most double labeling of SV2 and NTPDase1 in the inner synaptic layers appears closely intercalated but not overlapped, which indicates mainly a postsynaptic and, hence, dendritic distribution of the enzyme in GC (Figs. 1G–1I). Simultaneous immunostaining with mN1-kaly and glutamine synthetase demonstrates that NTPDase1 is not present in Müller glia (Figs. 2A–2C). In contrast, RT97- and mN1-kaly-IR share a common pattern, which indicates that NTPDase1 is

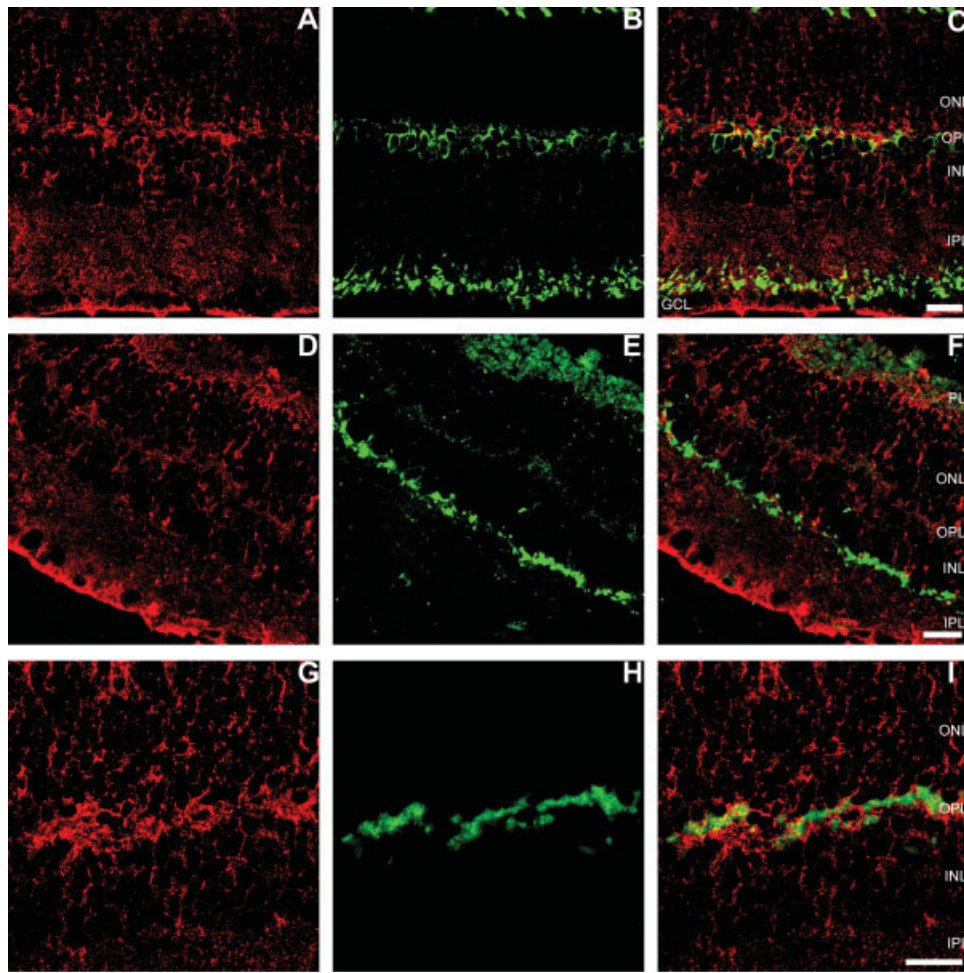


Fig. 3. Confocal microscope images of transverse sections from mouse retinas. NTPDase2 immunoreactivity (IR) is labeled red (A, D, G) and retinal markers are shown in green. Panel B depicts PKC α/β -labeled ON bipolar cells. Image E shows immunoreactivity for tyrosine hydroxylase (TH), which labels dopaminergic amacrine cells, and H depicts PSD95-labeled photoreceptor feet. Absence of

colabeling of NTPDase2-IR with TH or PSD-95 is observed in C and F. Image I shows partial colocalization between NTPDase2 and the ON bipolar cell marker. PL, photoreceptor layer; ONL, outer nuclear layer; OPL, outer plexiform layer; INL, inner nuclear layer; IPL, inner plexiform layer; GCL, ganglion cell layer. Images in the same row show identical magnification depicted by scale bars = 20 μm .

mainly restricted to horizontal cell processes in the OPL (Figs. 2D–2F). The ecto-enzyme immunostaining pattern (Fig. 2G) and colocalization with RT97-labeled GC axons (Fig. 2H) give further evidence that NTPDase1 is also highly expressed in optic fiber bundles. Immunostaining is also observed surrounding perikarya as well as proximal dendrites of GC. Retinal structures that appear to be vascular vessels also showed NTPDase-IR (Figs. 2A and 2I).

NTPDase2 in the mouse retina

In Figures 3A, 3D, and 3G, immunostaining with mN2–36 antibody in retinal sections displays a regular distribution throughout almost all retinal layers. In the outer retina, labeling is less confined than the one described for NTPDase1 and appears to surround

horizontal cells, spread throughout the OPL, and in lesser degree outer nuclear layer (ONL) cell bodies. In the INL there is also a dim labeling around cell somas. The IPL also presents a scattered but fainter pattern compared to the one observed for NTPDase1. Finally, the border of the vitreal surface exhibits a strong IR for NTPDase2, with a continuous distribution. Double immunostaining with mN2–36 and anti-PKC α/β antibodies shows only a sparse colocalization for these markers in the OPL and outer INL, indicating that this enzyme subtype might be scarcely expressed in ON rod bipolar cell membranes (Figs. 3A–3C). In Figures 3D–3F, TH was used to evaluate if NTPDase2 was located in dopaminergic amacrine cell processes positive for tyrosine hydroxylase. This staining appears as puncta surrounding horizontal cell somas in the OPL as well as in the outermost

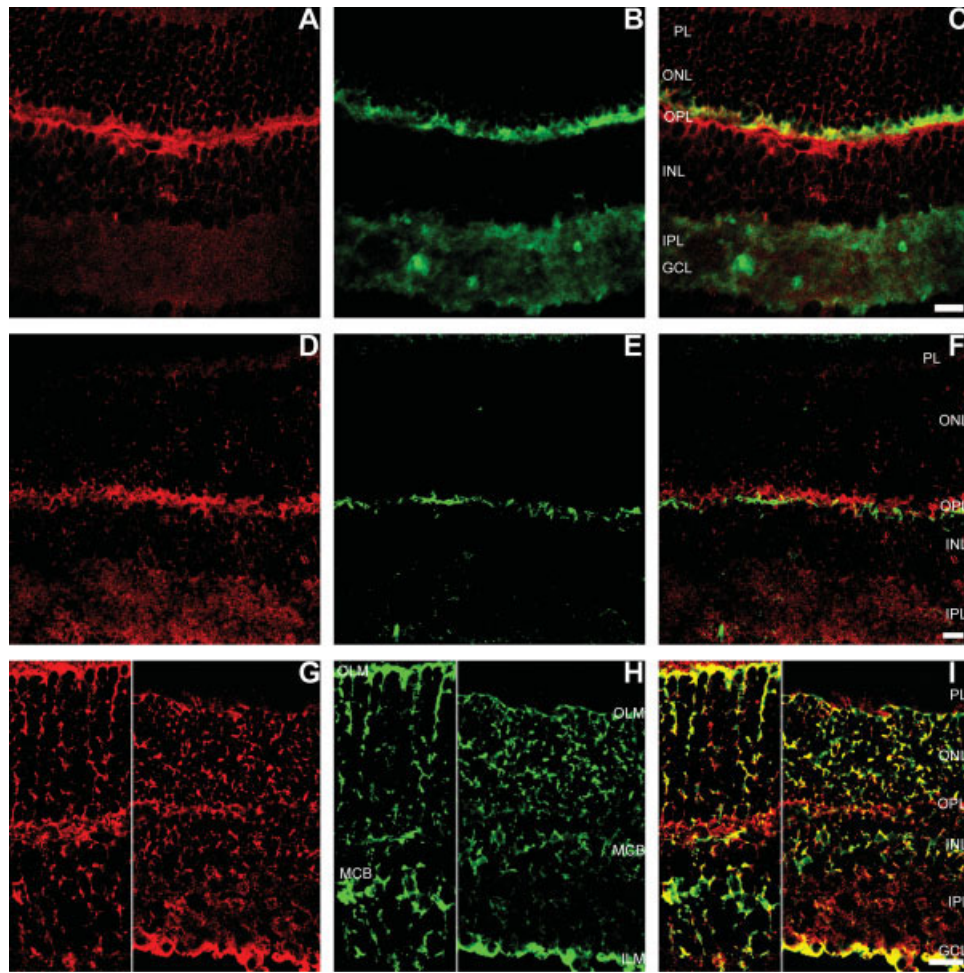


Fig. 4. Confocal microscope images of transverse sections from mouse retinas. NTPDase2 immunoreactivity (IR) is labeled red (A, D, G) and retinal markers are shown in green. Image in B depicts SV2-labeled presynaptic vesicles in the outer (OPL) and inner plexiform layers (IPL). RT97 labeled horizontal cell processes and glutamine synthetase (GS) labeled Müller cells, as shown in E and H, respectively. Analysis of overlaid images (C, F) indicates a limited colocalization of NTPDase2 with the presynaptic marker but its ab-

sence from horizontal cell processes in the OPL. In panel I, a conspicuous colabeling of NTPDase2-IR and GS-labeled Müller cells can be observed. Insets in the left side of panels G, H, and I show magnified images from a different retinal section. OLM, outer limiting membrane; MCB, Müller cell bodies; ILM, inner limiting membrane; PL, photoreceptor layer; ONL, outer nuclear layer; INL, inner nuclear layer; GCL, ganglion cell layer. Images in the same row show identical magnification. Scale bars = 20 μ m.

part of the IPL as described elsewhere (Haverkamp and Wässle, 2000). The absence of colocalization rules out the presence of NTPDase2 in the dopaminergic amacrine cell processes. Furthermore, mN2-36-IR is adjacent but not at all coincident with PSD95 staining in the OPL, which suggests that NTPDase2 is not expressed in rod and cone terminals (Figs. 3G–3I). SV2 and mN2-36 double labeling as illustrated in Figures 4A–4C, indicates some presynaptic staining in the OPL; however, NTPDase2 seems mainly located in the postsynaptic region. Moreover, red dots in the IPL appear to surround the green staining, suggesting a neighboring but not overlapping distribution between NTPDase2 and the presynaptic vesicle marker. Figures 4D–4F depict RT97 marker, which does not colocalize with mN2-36 labeling suggesting

that, in contrast to NTPDase1, NTPDase2 is not located in HC processes or GC axons. Noteworthy, as illustrated in Figures 4G–4I, mN2-36-IR shows a remarkable coincident pattern of distribution with GS immunostaining. This double labeling experiment demonstrates an almost complete and restricted expression of NTPDase2 by Müller glia, with the exemption of noncoincident labeling in the IPL and OPL. The NTPDase2 distribution seems to encompass Müller cell bodies from inner to outer limiting membranes.

NTPDase1 in the zebrafish retina

Figures 5A, 5D, and 5G as well as 6A and 6D show IR for mN1-kaly antibody, which labels several retinal

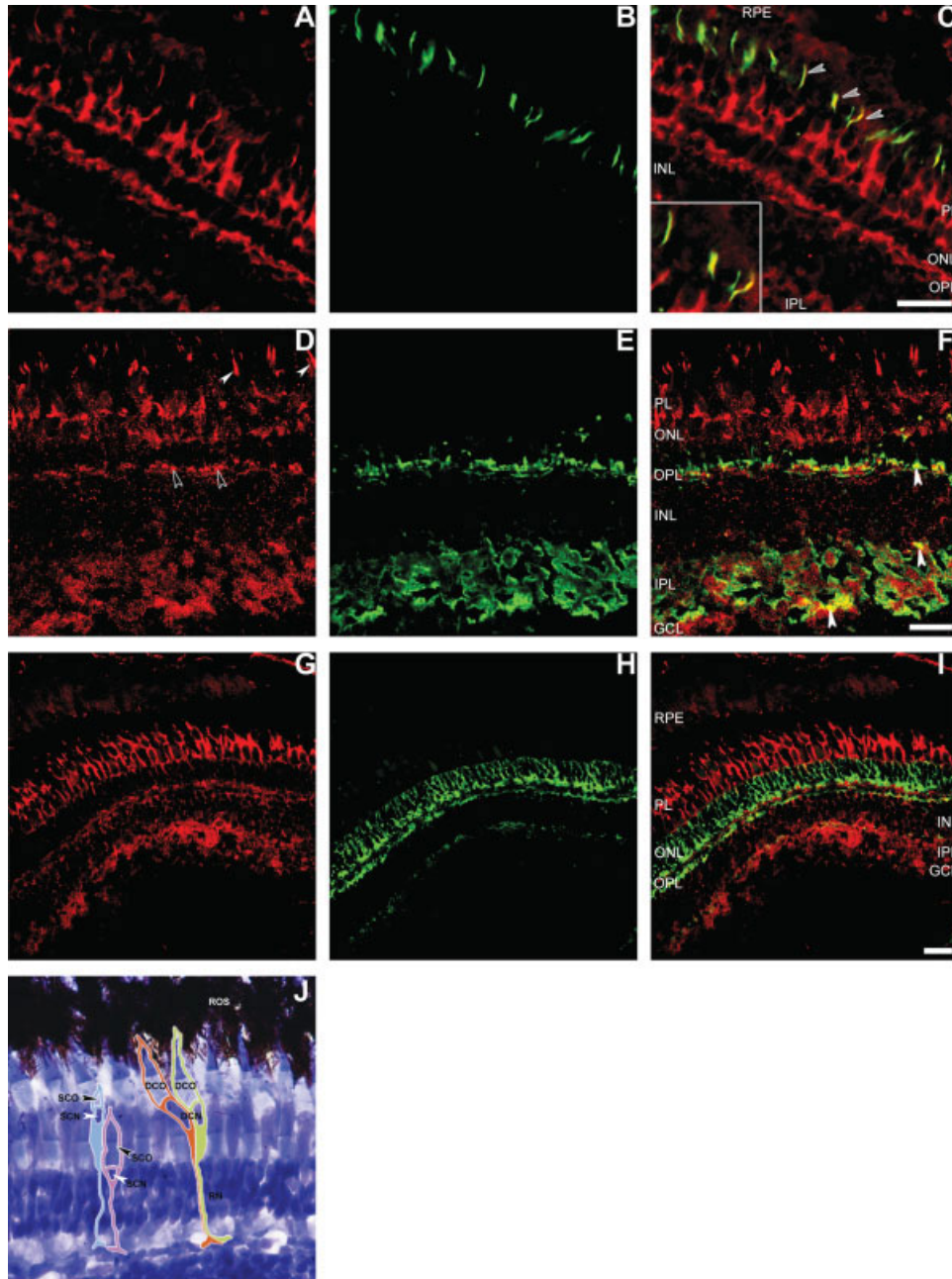


Fig. 5. Confocal microscope images of transverse sections from zebrafish retinas. NTPDase1 immunoreactivity (IR) is labeled red (A, D, G), while retinal markers are depicted in green. NTPDase1 appears regionalized in the photoreceptor layer (PL), outer and inner plexiform layers (OPL and IPL), ganglion cell layer (GCL), and retinal pigmented epithelium (RPE). White arrowheads in panel D show NTPDase1-IR in cone outer segments, while open arrowheads point to crescent-shaped NTPDase1 immunostaining in the OPL. Panel B depicts RT97-labeled photoreceptor outer segments. Panel E shows SV2-labeled presynaptic vesicles in the OPL and IPL. Zns-2-labeled cone pedicles and horizontal cell bodies are shown in image H. Panel J depicts a Nissl staining of a retinal section from zebrafish with a superimposed scheme, which was drawn

by us on a photomicrograph from a section of a zebrafish retina based on the scheme from the work of Fadool and Dowling (2008), illustrating double and single cones outline in the photoreceptor layer (PL), outer nuclear layer (ONL) and OPL. Panel C depicts colocalization of NTPDase1-IR and RT97-labeled photoreceptor outer segments (gray arrowheads and inset). Partial colocalization of NTPDase1 with the presynaptic marker in the outer and inner synaptic layers is shown in F (arrowheads). Image I depicts the absence of NTPDase1 from either cone terminals or horizontal cell bodies. DCO, double cone outer segments; DCN, double cone nuclei; SCN, single cone outer segments; SCN, single cone nuclei; ROS, rod outer segments; RN, rod nuclei; INL, inner nuclear layer. Images in the same row present identical magnification. Scale bars = 20 μ m.

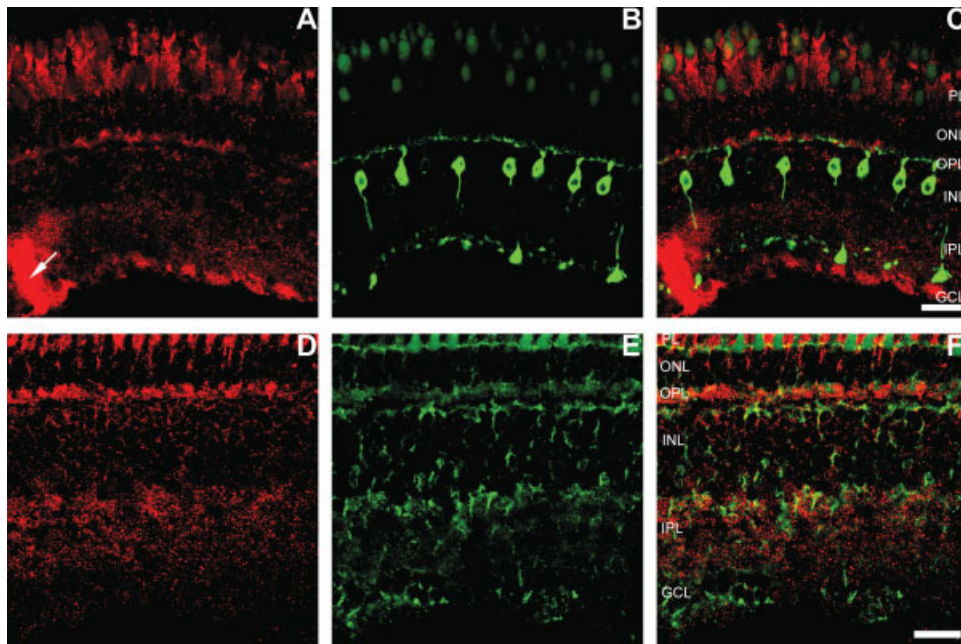


Fig. 6. Confocal microscope images of transverse sections from zebrafish retinas. NTPDase1 immunoreactivity (IR) is labeled red (A, D), while PKC α / β -labeled ON bipolar cells (B) as well as glutamine synthetase-labeled Müller glia (E) are shown in green. Panels C and F are superimposed images from each row. NTPDase1 does not colocalize with any of these markers immunoreactivity. In image

A, the arrow indicates a strong NTPDase1 immunostaining in a section of the optic nerve. PL, photoreceptor layer; ONL, outer nuclear layer; OPL, outer plexiform layer; INL, inner nuclear layer; IPL, inner plexiform layer; GCL, ganglion cell layer. All images exhibit identical magnification. Scale bar in F = 20 μ m.

layers with different intensity. Among the stained layers there is a clear labeling in the outermost part of the rod ONL, which appears to be positioned on single and double cone somas extending to their segments (Fig. 5D). Labeling with a more diffuse appearance is observed on rod outer segments and the RPE. Since eyecups were prepared from light-adapted zebrafish, cellular processes from the two epithelia are intertwined obscuring the analysis of the immunostaining. IR using anti-RT97 (which in zebrafish retinas labeled photoreceptor outer segments) and mN1-kaly antibodies indicates that the observed immunostaining is located at least in some single and double cone outer segments (Figs. 5A–5C); however, we cannot rule out the presence of NTPDase1 in the rod outer segments as well (Fig. 5D). In the OPL, labeling appears to be regionalized in crescent shaped structures. Sparser and dotted staining surrounds the edge of some but not all interneuron bodies in the INL. Similarly to the mouse retina, a more densely distributed labeling is present throughout the IPL and extends to the ganglion cell layer (GCL). Using anti-SV2 antibody in double labeling experiments (Figs. 5D–5F), we observed that mN1-kaly staining in the OPL shows a scant overlap with the presynaptic vesicle marker. In the IPL, almost no colocalization was observed, suggesting that NTPDase1 exhibits a major postsynaptic distribution in both synaptic

layers (Fig. 5F). Zns-2 antibody, a marker for cone photoreceptors in the zebrafish, also labels either rod periphery or Müller cell processes in the ONL as well as horizontal cell bodies (Yazulla and Studholme, 2001). In our retinal sections, zns-2 antibody labeled cone pedicles but not cone inner segments. Double labeling assays with Zns-2 antibody revealed that mN1-kaly-IR appears to be concentrated surrounding rod and double cone inner segments (Figs. 5G–5J and 6F). Furthermore, the crescent shaped structures in the OPL although closely associated do not colocalize with cone terminals (Figs. 5I and 7L). Figures 6A–6C depict that there is no overlap between NTPDase1 staining and all labeled ON bipolar cell processes or somas. mN1-kaly immunolabeling also appears in the GC axons. On the other hand, mN1-kaly staining does not colocalize with GS-IR, suggesting that NTPDase1 is not expressed by Müller glia (Figs. 6D–6F).

NTPDase2 in the zebrafish retina

Immunostaining with mN2-36 appears conspicuously regionalized in the OPL of the zebrafish retina as shown in Figure 7A. Labeling is punctate and fainter throughout the IPL and photoreceptor layer. Double labeling experiments with RT97 indicate that NTPDase2 it is expressed in rod and cone inner seg-

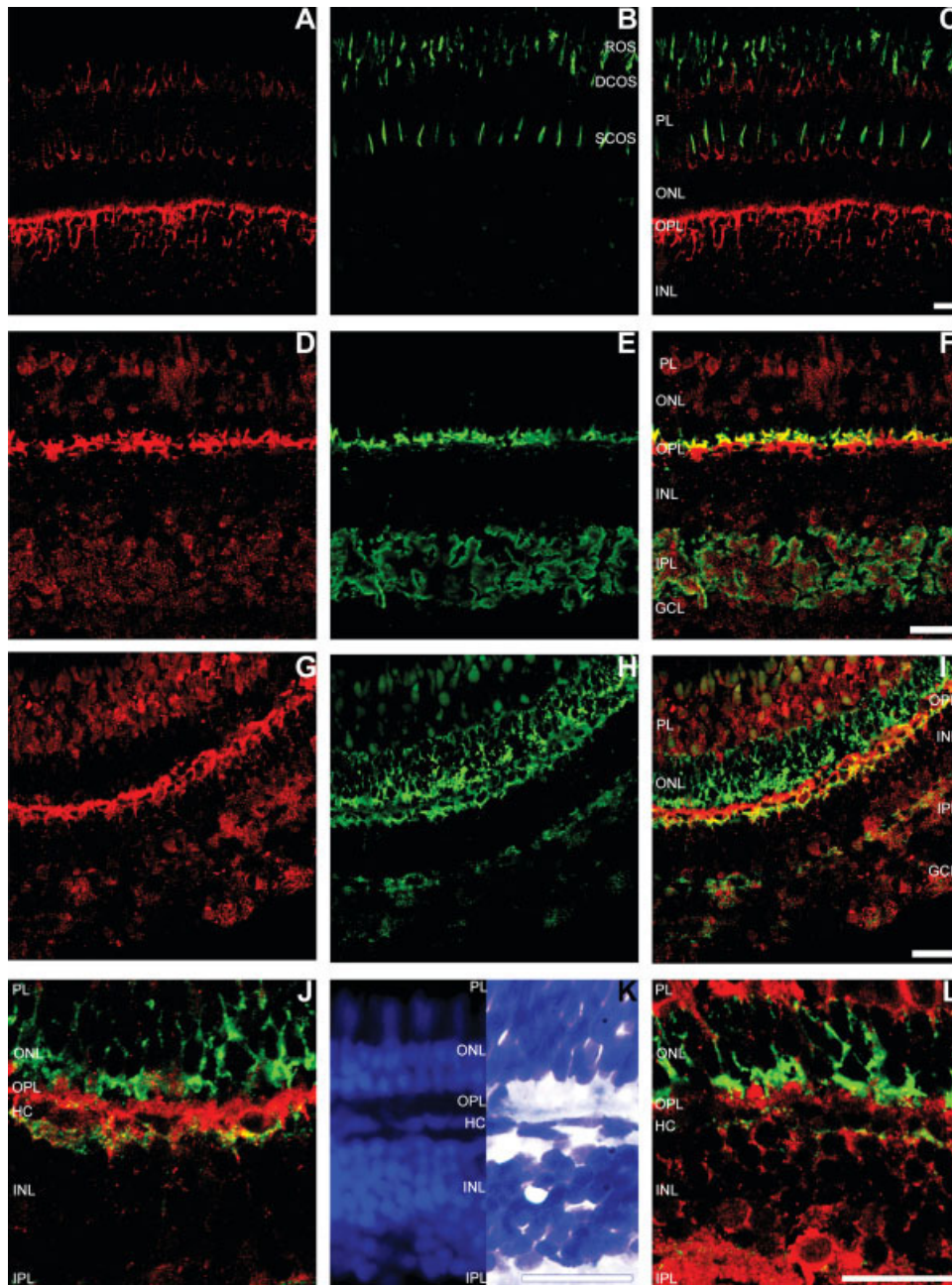


Fig. 7. Confocal microscope images of transverse sections from zebrafish retinas. NTPDase2 immunoreactivity (IR) is labeled red (A, D, G) and retinal markers are depicted in green. NTPDase2-IR is mostly distributed in the outer plexiform layer (OPL) but labeling in the photoreceptor layer (PL) and inner plexiform layer (IPL) is also apparent. Image B shows RT97-labeled photoreceptor outer segments. SV2-labeled presynaptic vesicles in the OPL and IPL and *zns-2*-labeled cone pedicles are shown in panels E and H, respectively. Overlaid images from each row are displayed in the third column. In panel C, adjacent labeling suggests the presence of NTPDase2 in photoreceptor inner segments. Image F displays colocalization between NTPDase2- and SV2-IR in the OPL. Panel I

depicts absence of colocalization of NTPDase2 in cone terminals, but a partial colocalization in horizontal cell bodies. Images in the bottom row are a magnified detail of overlaid images showing *zns-2*-IR and either NTPDase2 (panel J) or NTPDase1 (panel L) staining. Image K shows a transverse section of a zebrafish retina stained with Hoechst (left) or Nissl (right). ONL, outer nuclear layer; HC, horizontal cells; INL, inner nuclear layer; GCL, ganglion cell layer; DCOS, double cone outer segments; SCOS, single cone outer segments; ROS, rod outer segments. Images in the same row share the same magnification unless indicated by the presence of a different scale bar. Scale bars = 20 μ m.

ments though not expressed by photoreceptor outer segments (Figs. 7A–7C). There is also scattered staining around perikarya in the outer half of the INL. Double labeling with SV2 shows partial colocalization,

which may indicate that NTPDase2 is expressed both pre- and postsynaptically in the OPL. In the IPL, in contrast, all staining for the enzyme seems to be postsynaptic and extends to the GCL (Figs. 7D–7F). *Zns-2*

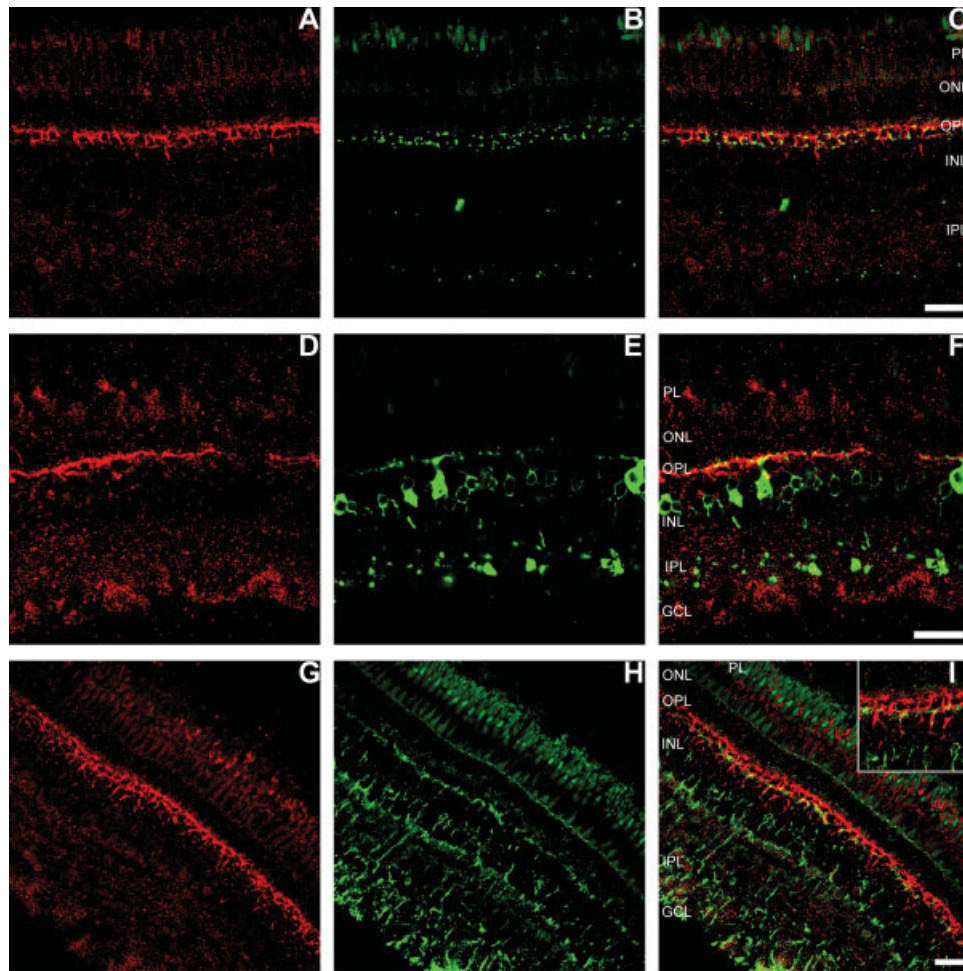


Fig. 8. Confocal microscope images of transverse sections from zebrafish retinas. NTPDase2 immunoreactivity (IR) is labeled red (A, D, G) and retinal markers are displayed in green. Panel B shows tyrosine hydroxylase (TH)-labeled interplexiform amacrine cell processes in the outer plexiform layer (OPL). Image E illustrates PKC α/β -labeled ON bipolar cells. In panel H, glutamine synthetase (GS)-IR reveals Müller cells. Overlaid images demonstrate the absence of colocalization between NTPDase2 and either TH-

(panel C) or GS-labeled cells (panel I and inset, which shows a magnified view of the OPL region). In contrast, there is partial colabeling of NTPDase2 with PKC α/β -IR (F). PL, photoreceptor layer; ONL, outer nuclear layer; INL, inner nuclear layer; IPL, inner plexiform layer; GCL, ganglion cell layer. All images (except inset) share the same magnification indicated in panel I. Scale bars = 20 μ m.

and mN2-36-IRs shown in Figures 8G–8I, and analyzed together with Nissl and Hoechst staining of the same area (Figs. 7J and 7K), suggest that NTPDase2 presence in the OPL is restricted to HC bodies and processes. However, this ecto-enzyme subtype could be at least in part localized in amacrine interplexiform cell processes. To further investigate mN2-36-IR in the OPL a double labeling experiment with anti-TH antibody was performed. Results illustrated in Figures 8A–8C show that labeling corresponding to NTPDase2 is not localized in dopaminergic interplexiform cell processes surrounding horizontal cells. In addition, we found that NTPDase2 immunostaining exhibits some degree of colocalization with ON bipolar cell dendrites labeled in the OPL (Figs. 8D–8F). We frequently found mN2-36-IR in the nerve fiber layer

(Fig. 8D). Finally, unlike mouse, Müller cells in the zebrafish do not seem to express NTPDase2 (Figs. 8G–8I).

NTPDases1 and 2 at the proliferative margin of the zebrafish retina

Zebrafish retina is endowed with a rim of tissue called margin germinal zone (MGZ), which contains proliferative and differentiating cells at the periphery of the mature more central retina. Cells located in the MGZ and positive for BrdU shown in Figure 9 are either mitotically active or recent postmitotic precursors. NTPDase1 and NTPDase2 are expressed within the MGZ including areas that closely surround BrdU-positive nuclei.

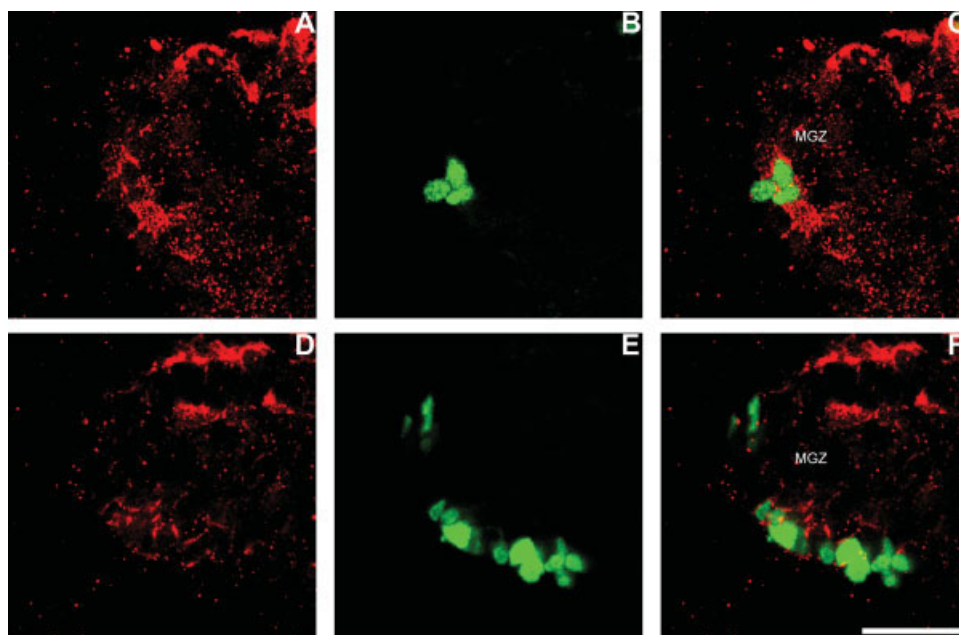


Fig. 9. Confocal microscope images of transverse sections from zebrafish retinas. NTPDase1 and NTPDase2 immunoreactivity is shown in red (A and D, respectively). Panels B and E depict 5-bromo-2'-deoxyuridine (BrdU) immunostaining for proliferative cell nuclei present in the margin germinal zone (MGZ) of the zebrafish

retina. The third column depicts overlaid images revealing the presence of both NTPDases immunostaining surrounding BrdU-labeled nuclei (C, F). All images share the same magnification indicated by scale bar in F = 20 μ m.

ATPase activity in mouse and zebrafish retinas

Figures 10A (mouse) and 10B (zebrafish) illustrate representative experiments of the production of Pi from ATP using neural retina homogenates. In the absence of inhibitors (ATPase activity), the rate of Pi production expressed as $\text{nmol}/(\mu\text{g protein}\cdot\text{min})$ was $v_{i_T} = 0.0545 \pm 0.0066$ ($n = 4$) for mouse and $v_{i_T} = 0.0145 \pm 0.0075$ ($n = 4$) for zebrafish. In the presence of both ion-pump ATPases and phosphatase inhibitors, ecto-ATPase activity amounted to $v_{i_E} = 0.035 \pm 0.0014$ ($n = 4$) for mouse and $v_{i_E} = 0.0092 \pm 0.0050$ ($n = 5$) for zebrafish. For both vertebrate species, about 60% of total ATP hydrolysis can be assigned to ecto-ATPase activity. In assay media with 10 mM of either EDTA or Cibacron blue there was no production of Pi, that is, the remaining Pi production in the presence of the ion-pump ATPases and phosphatase inhibitors was completely abolished. Thus, the reported v_{i_E} defines a calcium-dependent ecto-ATPase activity that may be owed at least to NTPDases1 and 2 identified by immunocytochemistry in this report.

DISCUSSION

In the present report we show a detailed immunocytochemical characterization of the distribution of NTPDases1 and 2 in cellular and synaptic layers of the retina from mouse and zebrafish, two phylogenetically distant species of vertebrate.

NTPDase2 localization in the retina of mouse

Expression of NTPDases1, 2, and 3 has been reported in the nervous system of vertebrates (Massé et al., 2006; Rico et al., 2003, 2006; Smith and Kirley, 1998; Vljakovic et al., 2002; Vorhoff et al., 2005; Zimmermann, 1996; Zimmermann and Braun, 1999). A recent report described the presence of NTPDase2 in Müller cell membranes of the rat retina (Iandiev et al., 2007). Moreover, an ecto-ATPase activity associated to both OPL and IPL has been described in the retina of rat (Puthusserly and Fletcher, 2007). Similarly, in the mouse retina we found NTPDase2 to be principally localized in radial Müller glia and dendrites of GC in the inner plexiform layer, suggesting that ATP, which is released by astrocytes and Müller glia as well as by GCs (Newman, 2006), might be hydrolyzed both auto-crinally and paracrinally in the IPL and GCL. We also observed immunostaining in the outer plexiform (synaptic) layer, but we cannot discriminate whether NTPDase2 is also present in interneuron processes, not labeled by any of the markers we have used, or in Müller glia processes that do not contain glutamine synthetase. NTPDase2 expression in Müller cells was not restricted to the inner retina but extended throughout the radial Müller glia suggesting that nucleotides, perhaps released from various retinal sources, including the outer retina, can be hydrolyzed by NTPDase2. The presence of NTPDase2 on Müller cells and synaptic layers may terminate the action of ATP on P2X iono-

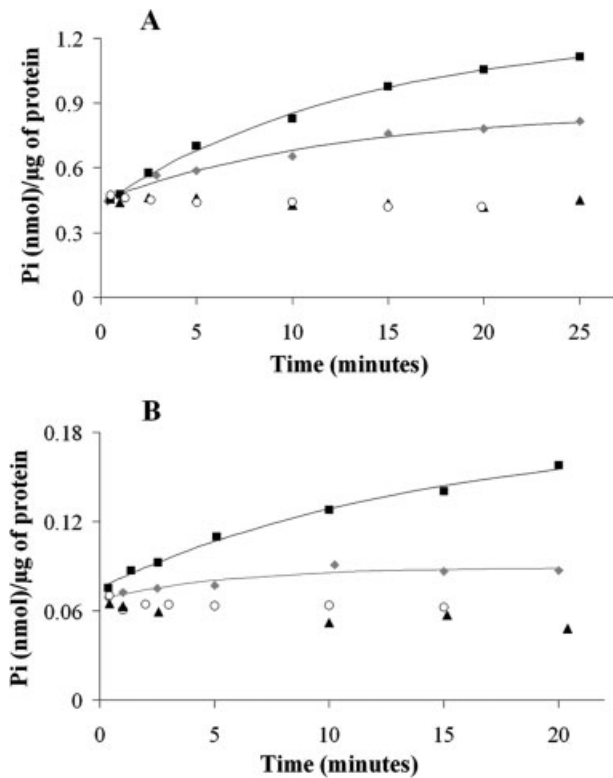


Fig. 10. ATPase activity in retinal homogenates of mouse (A) and zebrafish (B). Inorganic phosphate production was followed at different intervals after adding [γ - 32 P]ATP to the tissue homogenate (time 0). Squares represent ATPase activity in the absence of inhibitors. Ecto-ATPase activity was measured in the presence of ion-pump ATPases and alkaline phosphatase inhibitors (diamonds). [γ - 32 P]Pi production in the presence of 10 mM either EDTA or cibacron blue was not detected (triangles and circles, respectively). Curved lines depict the best fit of a single exponential function to experimental data. A representative experiment from four to five independent measurements is shown for each species.

tropic receptors and increase extracellular levels of ADP which in turn might activate G protein-coupled P2Y receptors (Burnstock, 2007). Considering other nucleotides, NTPDase2 presence and activity in the retinal compartments described here could favor UDP accumulation in the extracellular milieu (Kukulski et al., 2005).

NTPDase1 localization in the retina of mouse

NTPDase1 is usually associated with the microglia and the vasculature of the brain (Braun et al., 2000; Braun and Zimmermann, 2001). Accordingly, we observed conspicuous NTPDase1-IR in the choroid as well as in structures which look like intraretinal blood vessels in the outer and inner synaptic layers. In contrast to NTPDase2, NTPDase1 is not expressed by Müller cells in the mouse retina, which is in agreement with data observed in the rat retina (Iandiev et al., 2007). The report also indicates that NTPDase1 is not expressed by neural cells in the rat retina. In

contrast, we observed that NTPDase1 is located on neurons in the mouse retina, since it is expressed by postsynaptic HC processes in the OPL and GC dendrites in the IPL. We cannot ascertain the basis for the observed dissimilarities, but they might be due to the use of antibodies against NTPDase1 with different specificity, species-specific distribution of NTPDase1, or differential detection sensitivity of the methodological procedure used.

The presence of NTPDase1 in HC may indicate regulation of the extracellular concentration of nucleotides originated from photoreceptor terminals and/or released by Müller cells in the outer synaptic layers. In our study, NTPDase1 is also expressed by axons of GCs in the nerve fiber layer. In this layer, NTPDase1 might also be expressed by microglia or astrocytes, which have been shown to harbor P2X receptors (Bianco et al., 2005; Xiang and Burnstock, 2005) and to release ATP (Newman, 2006). The regionalized presence of NTPDase1 would suggest a rapid hydrolysis of both ATP and ADP released in the vicinity of the enzyme, limiting the activation of P2 receptors and quickly rising extracellular AMP concentration. The latter molecule, in turn, becomes available as a substrate for adenosine synthesis.

Localization of NTPDase1 and NTPDase2 in the retina of zebrafish

Phylogenetic analyses of amino acid conservation have shown that members of the E-NTPDase family are conserved among vertebrates and each particular NTPDase shares a higher degree of identity among species than different NTPDases within the same species (Massé et al., 2006). NTPDases 1, 2, and 3 have been cloned and their mRNA expression reported to be present in the adult brain as well as the spinal cord, cranial ganglia, and hypothalamus of the zebrafish embryo (Appelbaum et al., 2007; Rico et al., 2006). The polyclonal antibodies against NTPDase1 and NTPDase2 we used appear to consistently identify two different proteins in the adult zebrafish retina, since their expression pattern did not overlap. Likewise, NTPDase1 is not expressed by photoreceptor terminals or bipolar cells, whereas NTPDase2 seems to be expressed by rod but not cone pedicles as well as by dendrites of bipolar cells in the OPL. Both NTPDases (1 and 2) are predominantly located postsynaptic to photoreceptor cells, principally in HC, although their staining patterns are essentially different. In fact, NTPDase2 densely surrounds horizontal cell bodies and proximal cell processes, while NTPDase1 distribution closely resembles the glutamate receptor GluR2 staining pattern on distal tips of HC dendrites just beneath cone synaptic terminals in the retina of zebrafish (Shields et al., 2007). Besides, NTPDase2 pattern in the outer synaptic layer looks like the IR pattern for the GABA C receptor ρ subunit, which surrounds hor-

izontal cell bodies with processes extending to the OPL (Yazulla and Studholme, 2001). In our immunostaining, NTPDase2 labeling extends from HC bodies to delineate interneuron somas in the INL as well. Furthermore, we cannot rule out the possibility that NTPDases1 and 2 are expressed by different subpopulations of HC (Song et al., 2008). The presence of both NTPDases in the outer synaptic layer suggests that nucleotides would be regulated in a different manner according to the type of NTPDase they encounter in or near their site of release. We also observed NTPDase1 immunostaining in photoreceptor outer and inner segments, which indicates that photoreceptor cells might have the ability of hydrolyzing nucleotides originated in the RPE and released to the subretinal space between the pigmented epithelium and photoreceptors (Lu et al., 2007; Mitchell, 2001). The observation that NTPDase1 seems to be present in the RPE is consistent with studies describing the presence of ecto-ATPase activity as well as mRNA for NTPDases1 to 3 in cultured RPE cells (Reigada et al., 2005). Regarding retinal inner layers, both enzyme subtypes are expressed in dendrites and axons of GCs where they could be able to differentially regulate synaptic transmission and/or Müller glia-neuron purinergic-mediated interactions (Newman, 2006), as it was suggested earlier for the mouse retina.

NTPDases are expressed within neurogenic areas of the zebrafish retina

Taking into consideration that purine nucleotides play important roles during development from the moment of fertilization (Laasberg, 1990) and NTPDase2 is essential for the morphogenesis of the eye and retina in *Xenopus* embryos (Massé et al., 2007), we looked for NTPDase1 and NTPDase2 expression in the neurogenic border (MGZ) of the adult zebrafish retina, where cells develop from pluripotent precursors to differentiated neurons and Müller glia (Raymond et al., 2006). We observed that both NTPDases1 and 2 are expressed surrounding either just postmitotic or still proliferating cells. NTPDase2 has been previously associated to precursor cells like type-B astrocytes and radial glia-like cells in several neurogenic areas of the adult rat brain (Braun et al., 2003; Shukla et al., 2005). The kind of progenitor cell expressing these enzymes and whether each enzyme subtype is associated to different subpopulations of progenitor cells are open questions that deserve further investigation. So far, our results suggest that, in the adult zebrafish retina, both NTPDases studied are expressed within zebrafish MGZ.

Ecto-ATPase activity

E-NTPDases are able to hydrolyze nucleoside triphosphates and diphosphates and are insensitive to inhibitors of both ion-pump ATPases and phosphatases (Plesner, 1995). As E-NTPDase activity is de-

pendent on either Ca^{2+} or Mg^{2+} , inhibition of the ecto-ATPase activity by divalent cation chelator molecules provides further evidence that the observed activity might be due to NTPDases. Moreover, E-NTPDase activity should be blocked by the nucleotide analog cibacron blue (Chen et al., 1996; Munkonda et al., 2007). We detected ecto-ATPase activity in retinal homogenates from both species, in the presence of the aforementioned inhibitors. Similar to other cell systems, the observed ecto-ATPase activity was completely blocked either with cibacron blue or in divalent cations-free medium (Nagy et al., 1986). Absolute values for ecto-ATPase activity lie in the range of that found for homogenates of goldfish retina [v_{i_T} : 0.030 ± 0.0036 and v_{i_E} : 0.017 ± 0.0025 nmol/(μg protein min)] as well as other nonneural tissues in mouse (Sévigny et al., 2002), although zebrafish retinal values were significantly lower than ecto-ATPase activity reported for zebrafish brain homogenates (Rico et al., 2003). Nevertheless, comparisons of absolute values are difficult to assess, since enzymatic reaction conditions as well as tissue preparations differ considerably among studies. The observed ecto-ATPase activity both in mouse and zebrafish retina might be owed at least to NTPDases1 and 2, whose expression we have described by immunocytochemistry in this report.

Further considerations

Certainly, the physiological picture appears much more complex, since NTPDase3 as well as other ectonucleotidases, which are not addressed in this report, may also be present in the retinal circuitry of both species. Therefore, the extracellular concentration of nucleotides, at each time, will result from the fine-tuning of several ecto-enzyme orchestrated activities, which can be present in the extracellular microenvironment where ATP as well as other nucleotides are released. However, a compartmentalized distribution of NTPDases1 and 2 suggests a relevant role for these enzymes in controlling nucleotide levels and the intracellular transduction mechanisms activated by these molecules in the physiology of the vertebrate neural retina.

ACKNOWLEDGMENTS

Monoclonal antibodies zns-2, SV2, and RT97 developed by Dr. Bill Trevarrow (Institute of Neuroscience, University of Oregon), Dr. Kathleen Buckley (Department of Neurobiology, Harvard Medical School), and Dr. John Wood (Sandoz Institute for Medical Research, London) were obtained from the Developmental Studies Hybridoma Bank, developed under the auspices of the NICHD and maintained by the University of Iowa, Department of Biological Sciences, Iowa City, IA. TH and GS antibodies were a kind gift

from Dr. David Krizaj, Department of Ophthalmology, University of Utah, Salt Lake City, UT.

REFERENCES

- Adamus G, Zam ZS, McDowell JH, Shaw GP, Hargrave PA. 1988. A monoclonal antibody specific for the phosphorylated epitope of rhodopsin: comparison with other anti-phosphoprotein antibodies. *Hybridoma* 7:237–247.
- Anderton BH, Breinburg D, Downes MJ, Green PJ, Tomlinson BE, Ulrich J, Wood JN, Kahn J. 1982. Monoclonal antibodies show that neurofibrillary tangles and neurofilaments share antigenic determinants. *Nature* 1:84–86.
- Appelbaum L, Skariah G, Mourrain P, Mignot E. 2007. Comparative expression of p2x receptors and ecto-nucleoside triphosphate diphosphohydrolase 3 in hypocretin and sensory neurons in zebrafish. *Brain Res* 1174:66–75.
- Bianco F, Fumagalli M, Pravettoni E, D'Ambrosi N, Volonte C, Matteoli M, Abbraccio MP, Verderio C. 2005. Pathophysiological roles of extracellular nucleotides in glial cells: differential expression of purinergic receptors in resting and activated microglia. *Brain Res Brain Res Rev* 48:144–156.
- Braun N, Zimmermann H. 2001. Microglial ectonucleotidases: Identification and functional roles. *Drugs Dev Res* 53:208–217.
- Braun N, Sévigny J, Robson SC, Enjoji K, Guckelberger O, Hammer K, Di Virgilio F, Zimmermann H. 2000. Assignment of ecto-nucleoside triphosphate diphosphohydrolase-1/cd39 expression to microglia and vasculature of the brain. *Eur J Neurosci* 12:4357–4366.
- Braun N, Sévigny J, Mishra SK, Robson SC, Barth SW, Gerstberger R, Hammer K, Zimmermann H. 2003. Expression of the ecto-ATPase NTPDase2 in the germinal zones of the developing and adult rat brain. *Eur J Neurosci* 17:1355–1364.
- Burnstock G. 1972. Purinergic nerves. *Pharmacol Rev* 24:509–581.
- Burnstock G. 1978. A basis for distinguishing two types of purinergic receptors. In: Straub RW, Bolis L, editors. *Cell membrane receptors for drugs and hormones: A multidisciplinary approach*. New York: Raven Press. p 107–118.
- Burnstock G. 2007. Physiology and pathophysiology of purinergic neurotransmission. *Physiol Rev* 87:659–797.
- Cameron DA, Carney LH. 2000. Cell mosaic patterns in the native and regenerated inner retina of zebrafish: Implications for retinal assembly. *J Comp Neurol* 416:356–367.
- Chen BC, Lee CM, Lin WW. 1996. Inhibition of ecto-ATPase by PPADS, suramin and reactive blue in endothelial cells, C6 glioma cells and RAW 264.7 macrophages. *Br J Pharmacol* 119:1628–1634.
- Dowling JE. 1979. Information processing by local circuits: The vertebrate retina as a model system. In: Schmitt FO, Worden FG, editors. *Neurosciences: Fourth study program*. Cambridge, MA: MIT Press. p 163–181.
- Dräger UC, Edwards DL, Bamstable CJ. 1984. Antibodies against filamentous components in discrete cell types of the mouse retina. *J Neurosci* 4:2025–2042.
- Enjoji K, Sévigny J, Lin Y, Frenette PS, Christie PD, Esch JS, Imai M, Edelberg JM, Rayburn H, Lech M, Beeler DL, Csizmadia E, Wagner DD, Robson SC, Rosenberg RD. 1999. Targeted disruption of cd39/ATP diphosphohydrolase results in disordered hemostasis and thromboregulation. *Nat Med* 5:1010–1017.
- Fadool JM, Dowling JE. 2008. Zebrafish: A model system for the study of eye genetics. *Progress Retinal Eye Res* 27:89–110.
- Fausther M, Lecka J, Kukulski F, Levesque SA, Pelletier J, Zimmermann H, Dranoff JA, Sévigny J. 2007. Cloning, purification, and identification of the liver canalicular ecto-ATPase as NTPDase8. *Am J Physiol Gastrointest Liver Physiol* 292:G785–795.
- Fellin T, Sul JY, D'Ascenzo M, Takano H, Pascual O, Haydon PG. 2006. Bidirectional astrocyte-neuron communication: The many roles of glutamate and ATP. *Novartis Found Symp* 276:208–217; discussion 217–221, 233–207, 275–281.
- Freedholm BB. 1995. Purinoceptors in the nervous system. *Pharmacol Toxicol* 76:228–239.
- Greferath U, Grunert U, Wässle H. 1990. Rod bipolar cells in the mammalian retina show protein kinase C-like immunoreactivity. *J Comp Neurol* 301:433–442.
- Haverkamp S, Wässle H. 2000. Immunocytochemical analysis of the mouse retina. *J Comp Neurol* 424:1–23.
- Hunsucker SA, Mitchell BS, Spychala J. 2005. The 5'-nucleotidases as regulators of nucleotide and drug metabolism. *Pharmacol Ther* 107:1–30.
- Iandiev I, Wurm A, Pannicke T, Wiedemann P, Reichenbach A, Robson SC, Zimmermann H, Bringmann A. 2007. Ectonucleotidases in Müller glial cells of the rodent retina: Involvement in inhibition of osmotic cell swelling. *Purinergic Signal* 3:423–433.
- Inoue T, Hosokawa M, Morigiwa K, Ohashi Y, Fukuda Y. 2002. Bcl-2 Overexpression does not enhance in vivo axonal regeneration of retinal ganglion cells after peripheral nerve transplantation in adult mice. *J Neurosci* 22:4468–4477.
- Kaczmarek E, Koziak K, Sévigny J, Siegel JB, Anrather J, Beaudoin AR, Bach FH, Robson SC. 1996. Identification and characterization of CD39/vascular ATP diphosphohydrolase. *J Biol Chem* 271:33116–33122.
- Koulen P, Fletcher EL, Craven SE, Bredt DS, Wässle H. 1998. Immunocytochemical localization of the postsynaptic density protein PSD-95 in the mammalian retina. *J Neurosci* 18:10136–10149.
- Kukulski F, Lévesque SA, Lavoie EG, Lecka J, Bigonnesse F, Knowles AF, Robson SC, Kirley TL, Sévigny J. 2005. Comparative hydrolysis of P2 receptor agonist by NTPDase 1, 2, 3 and 8. *Purinergic Signal* 1:193–204.
- Laasberg T. 1990. Ca²⁺-mobilizing receptors of gastrulating chick embryo. *Comp Biochem Physiol C* 97:9–12.
- Larison K, Trevarrow B. 1994. Zebrafish monoclonal antibodies. In: Westerfield M, editor. *The zebrafish book*, 21st ed. Eugene, OR: University of Oregon Press.
- Lazarowski ER, Boucher RC, Harden TK. 2003. Mechanisms of release of nucleotides and integration of their action as P2X- and P2Y-receptor activating molecules. *Mol Pharmacol* 64:785–795.
- Lowry OH, Rosebrough NJ, Farr AL, Randall RJ. 1951. Protein measurement with the Folin phenol reagent. *J Biol Chem* 193–265.
- Lu W, Reigada D, Sévigny J, Mitchell CH. 2007. Stimulation of the P2Y1 receptor up-regulates nucleoside-triphosphate diphosphohydrolase-1 in human retinal pigment epithelial cells. *J Pharmacol Exp Ther* 323:157–164.
- Masland RH. 2001. The fundamental plan of the retina. *Nat Neurosci* 4:877–886.
- Massé K, Eason R, Bhamra S, Dale N, Jones EA. 2006. Comparative genomic and expression analysis of the conserved NTPDase gene family in *Xenopus*. *Genomics* 87:366–381.
- Massé K, Bhamra S, Eason R, Dale N, Jones EA. 2007. Purine-mediated signaling triggers eye development. *Nature* 449:1058–1062.
- Mishra SK, Braun N, Shukla V, Fullgrabe M, Schomerus C, Korf HW, Gachet C, Ikehara Y, Sévigny J, Robson SC, Zimmermann H. 2006. Extracellular nucleotide signaling in adult neural stem cells: synergism with growth factor mediated cellular proliferation. *Development* 133:675–684.
- Mitchell CH. 2001. Release of ATP by a human retinal pigment epithelial cell line: Potential for autocrine stimulation through sub-retinal space. *J Physiol* 534:193–202.
- Mulero JJ, Yeung G, Nelken ST, Ford JE. 1999. CD39-L4 is a secreted human apyrase, specific for the hydrolysis of nucleoside diphosphates. *J Biol Chem* 274:20064–20067.
- Munkonda MN, Kauffenstein G, Kukulski F, Levesque SA, Legendre C, Pelletier J, Lavoie EG, Lecka J, Sévigny J. 2007. Inhibition of human and mouse plasma membrane-bound NTPDases by P2 receptor antagonists. *Biochem Pharmacol* 74:1524–1534.
- Nagy AK, Shuster TA, Delgado-Escueta AV. 1986. Ecto-ATPase of mammalian synaptosomes: identification and enzymatic characterization. *J Neurochem* 47:976–986.
- Newman EA. 2006. A purinergic dialogue between neurons and glia in the retina. *Novartis Found Symp* 276:193–202; discussion 202–207, 233–237, 275–281.
- Newman EA, Zahs KR. 1998. Modulation of neuronal activity by glial cells in the retina. *J Neurosci* 18:4022–4028.
- Plesner L. 1995. Ecto-ATPases: identities and functions. *Int Rev Cytol* 158:141–214.
- Puthussery T, Fletcher EL. 2007. Neuronal expression of P2X3 purinoceptors in the rat retina. *Neuroscience* 146:403–414.
- Ramón y Cajal S. 1892. La retina des vertébrés. *La Cellule* 9:119–259.
- Raymond PA, Barthel LK, Bernardos RL, Perkowski JJ. 2006. Molecular characterization of retinal stem cells and their niches in adult zebrafish. *BMC Dev Biol* 6:36–52.
- Reigada D, Lu W, Zhang X, Friedman C, Pendrak K, McGlenn A, Stone RA, Latics AM, Mitchell CH. 2005. Degradation of extracellular ATP by the retinal pigment epithelium. *Am J Physiol Cell Physiol* 289:C617–C624.
- Rico EP, Senger MR, Fauth Mda G, Dias RD, Bogo MR, Bonan CD. 2003. ATP and ADP hydrolysis in brain membranes of zebrafish (*Danio rerio*). *Life Sci* 73:2071–2082.
- Rico EP, Rosemberg DB, Senger MR, Arizi Mda B, Bernardi GF, Dias RD, Bogo MR, Bonan CD. 2006. Methanol alters ecto-nucleotidases and acetylcholinesterase in zebrafish brain. *Neurotoxicol Teratol* 28:489–496.

- Schulte am Esch J 2nd, Sévigny J, Kaczmarek E, Siegel JB, Imai M, Koziak K, Beaudoin AR, Robson SC. 1999. Structural elements and limited proteolysis of CD39 influence ATP diphosphohydrolyase activity. *Biochemistry* 38:2248–2258.
- Schwarzbaum PJ, Frischmann ME, Krumschnabel G, Rossi RC, Wieser W. 1998. Functional role of ecto-ATPase activity in goldfish hepatocytes. *Am J Physiol* 274:R1031–1038.
- Sévigny J, Sundberg C, Braun N, Guckelberger O, Csizmadia E, Qawi I, Imai M, Zimmermann H, Robson SC. 2002. Differential catalytic properties and vascular topography of murine nucleoside triphosphate diphosphohydrolase 1 (NTPDase1) and NTPDase2 have implications for thromboregulation. *Blood* 99:2801–2809.
- Shields CR, Klooster J, Claassen Y, Ul-Hussain M, Zoidl G, Dermietzel R, Kamermans M. 2007. Retinal horizontal cell-specific promoter activity and protein expression of zebrafish connexin 52.6 and connexin 55.5. *J Comp Neurol* 501:765–779.
- Shukla V, Zimmermann H, Wang L, Kettenmann H, Raab S, Hammer K, Sévigny J, Robson SC, Braun N. 2005. Functional expression of the ecto-ATPase NTPDase2 and of nucleotide receptors by neuronal progenitor cells in the adult murine hippocampus. *J Neurosci Res* 80:600–610.
- Smith TM, Kirley TL. 1998. Cloning, sequencing, and expression of a human brain ecto-apyrase related to both the ecto-ATPases and CD39 ecto-apyrases1. *Biochim Biophys Acta* 1386:65–78.
- Song PI, Matsui JI, Dowling JE. 2008. Morphological types and connectivity of horizontal cells found in the adult zebrafish (*Danio rerio*) retina. *J Comp Neurol* 506:328–338.
- Trombetta ES, Helenius A. 1999. Glycoprotein reglucoxylation and nucleotide sugar utilization in the secretory pathway: Identification of a nucleoside diphosphatase in the endoplasmic reticulum. *Embo J* 18:3282–3292.
- Vlajkovic SM, Thorne PR, Sévigny J, Robson SC, Housley GD. 2002. NTPDase1 and NTPDase2 immunolocalization in mouse cochlea: Implications for regulation of p2 receptor signaling. *J Histochem Cytochem* 50:1435–1442.
- Vorhoff T, Zimmermann H, Pelletier J, Sévigny J, Braun N. 2005. Cloning and characterization of the ecto-nucleotidase NTPDase3 from rat brain: Predicted secondary structure and relations to members of the E-NTPDase family and actin. *Purinergic Signal* 1:259–270.
- Wang TF, Guidotti G. 1998. Widespread expression of ecto-apyrase (CD39) in the central nervous system. *Brain Res* 790:318–322.
- Wässle H, Riemann HJ. 1978. The mosaic of nerve cells in the mammalian retina. *Proc R Soc Lond B Biol Sci* 200:441–461.
- Xiang Z, Burnstock G. 2005. Expression of P2X receptors on rat microglial cells during early development. *Glia* 52:119–126.
- Yazulla S, Studholme KM. 2001. Neurochemical anatomy of the zebrafish retina as determined by immunocytochemistry. *J Neurocytol* 30:551–592.
- Zimmermann H. 1996. Biochemistry, localization and functional roles of ectonucleotidases in the nervous system. *Prog Neurobiol* 49:589–618.
- Zimmermann H. 2006. Ectonucleotidases in the nervous system. *Novartis Found Symp* 276:113–128; discussion 128–130, 233–237, 275–281.
- Zimmermann H, Braun N. 1999. Ecto-nucleotidases molecular structures, catalytic properties, and functional roles in the nervous system. *Prog Brain Res* 120:371–385.